Robust Planar Dynamic Pivoting by Regulating Inertial and Grip Forces

Yifan Hou, Zhenzhong Jia, Aaron M. Johnson, and Matthew T. Mason

Robotics Institute, Carnegie Mellon University
5000 Forbes Ave., Pittsburgh, PA 15213, USA
yifanh@cmu.edu, zhenzjia@cmu.edu, amj1@cmu.edu, matt.mason@cs.cmu.edu
http://mlab.ri.cmu.edu

Abstract. In this paper, we investigate the planar *dynamic pivoting* problem, in which a pinched object is reoriented to a desired pose through wrist swing motion and grip force regulation. Traditional approaches based on friction compensation do not work well for this problem, as we observe the torsional friction at the contact has large uncertainties during pivoting. In addition, the discontinuities of friction and the lower bound constraint on the grip force all make dynamic pivoting a challenging task for robots. To address these problems, we propose a robust control strategy that directly uses friction as a key input for dynamic pivoting, and show that active friction control by regulating the grip force significantly improves system stability. In particular, we embed a Lyapunov-based control law into a quadratic programming framework, which also ensures real-time computational speed and the existence of a solution. The proposed algorithm has been validated on our dynamic pivoting robot that emulates human wrist-finger configuration and motion. The object orientation can quickly converge to the target even under considerable uncertainties from friction and object grasping position, where traditional methods fail.

Keywords: Robot, Manipulation, Pivoting, Friction, Robust Control

1 Introduction

Compared with humans, robots have limited dexterity. In particular, certain tasks that are simple for humans can be quite challenging for robots. Beyond the dexterity of human hand, one important advantage of human manipulation is the use of a richer set of force resources (*extrinsic dexterity* [1]), including gravity, inertial forces, contact forces and friction. One such example is regrasping - to shift an object from one grasp pose to another. For robots, a common solution is to put the object on the ground or in a fixture, then move the robot hand to the desired pose and grasp again. The human hand, however, often employs a more direct approach: in-hand regrasp through arm, wrist, and finger motions without breaking contact.

In this paper, we study *dynamic pivoting* – a common nonprehensile regrasping manipulation. One example is shown in Fig. 1: the hand holds a cellphone

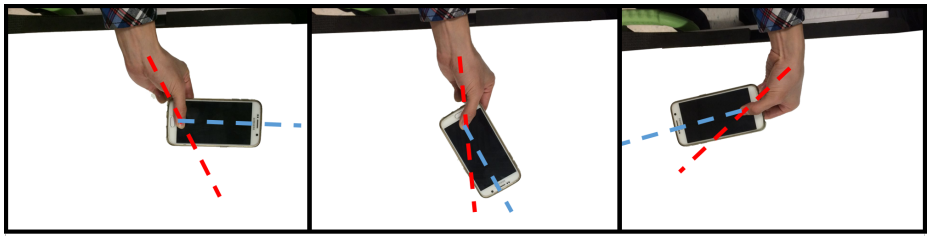

Fig. 1. Human pivots an in-hand object in the horizontal plane (top view).

between two finger tips, and rotates it to a desired angle relative to the finger by varying grip force and wrist rotation. Pivoting is a simple way to orient objects in the hand, and is faster than pick-and-place [2]. This operation is interesting because a human can modulate friction force and switch the contact mode between left sliding, right sliding and sticking, which is a hybrid control strategy.

This paper investigates techniques that enable a robot to perform human-like dynamic pivoting. The task is challenging for robots, because the contact brings three problems: [3–5].

The *Modeling Uncertainty*. On the one hand, we may not exactly know which area on the object is grasped, due to slipping or noise in the initial grasp. On the other hand, precise contact friction modeling is usually not realistic [6], so we have to tolerate some degree of uncertainty with practical friction models. Dynamic pivoting has even more frictional uncertainty due to noise in grip force control during fast motion. Recent work indicates that for certain robotic applications, a very detailed friction model is unnecessary [7–9]. However, a closed-loop strategy is preferred in these cases.

Positive lower bound constraint on grip force. We need a positive contact normal force to maintain grasping and reduce slip. In our preliminary simulations, however, a traditional nonlinear controller often commands large negative grip force when trying to pull the system back from error. If we truncate the grip force to satisfy the constraint, the traditional controller no longer works.

Friction discontinuity. We cannot assume a certain sliding direction, since the closed-loop system will need to fight against the position error in both directions during pivoting. As detailed in section 3.2, the stiction phenomenon introduces several different continuous modes, thereby directly introducing discontinuities into the gain matrix of the system.

In this work we propose a robust control strategy for robotic dynamic pivoting that addresses the above issues. A control law based on sliding mode control (SMC) calculates wrist torque and grip force within each continuous friction mode. The sliding condition, which leads to Lyapunov convergence, is imposed by a soft constraint and solved under control saturation as hard constraints. Following a hybrid system routine, when transition to multiple modes is possible, we add constraints to prevent undesired mode transitions when solving for a specific mode.

In particular, our algorithm:

- works with a discontinuous friction model;
- satisfies control saturation constraints including the positive lower bound;
- converges in experiments even when friction modeling are simplified and imprecise.

The paper is organized as follows. Section 2 describes the related work. Section 3 introduces the robotic pivoting system and modeling highlights. Section 4 presents the control strategy design. Section 5 presents the implementation and experimental results. Finally, Section 6 gives the summary and directions for future work.

2 Related Work

2.1 Pivoting

Rao *et al.* [10] were the first to use the term "pivoting" for the rotation of a grasped object relative to the contact point with fingers. Since there is no active joint at the contact, there must be an extrinsic source of actuation that drives the object, i.e. the *extrinsic dexterity* [1]. One such source is gravity [10, 2, 11, 9, 8, 12]. Brock calculated possible twists for an object in a multi-fingered hand under gravity by maximizing the virtual work [11]. Rao *et al.* [10], described how to choose a grasp so that after lifting up polyhedral objects from the ground, the object rotates to a desired stable pose under gravity. Holladay *et al.* [2], extended [10] by planning a whole trajectory for the gripper with the consideration of dynamics, and utilizing contact with the ground to discretize the final poses.

Gravity is a good source of actuation, for its perfectly precise direction and magnitude. The disadvantage is also obvious: its direction cannot change. We refer to those works as *gravity pivoting* in this paper.

Pivoting can be done by making contact with environment [1, 13]. We call them *contact pivoting*. Chavan-Dafle *et al.* implemented open-loop contact pivoting [13], where a firm grasp was maintained all the time during sliding. Contact pivoting is shown to be reliable in slow motion, as the object position can be inferred from the contact position.

We use inertial force as source of actuation, and call it *inertial pivoting*. Like gravity, inertial force does not rely on contact with the environment; however its direction is also controllable. Shi *et al.* [7], proposed an open-loop strategy for a three-DOF planar sliding problem, where an object grasped by a parallel gripper slides under inertial force and gravity. This strategy, though verified in simulation, showed notable error in experiments; the reason could be the lack of feedback, according to the authors. When the object is treated as an additional link of the robot with frictionless joint, pivoting reduces to a passive last joint manipulator problem, where partial feedback linearization is shown to be successful [14–18]. These approaches are extended in this paper in two ways. Firstly, we add a robust control term to the feedback linearization control law, so

as to explicitly tackle the non-trivial, uncertain contact friction and some amount of slip during pivoting. Secondly, we utilize the grip force as an additional source of control, which brings notable stability improvement as well as new difficulties in controller design.

There are very few studies using contact normal force to control friction directly, except for vibration suppression [19]. Closely related to our work, Via *et al.* [8, 9] performed controlled *gravity pivoting* to a spoon by controlling the grip force, and closed the loop with vision feedback. Robust control [8], and adaptive control techniques [9] were used to ensure convergence under friction uncertainty. They also improved the performance by adopting a more precise soft finger model. The controller was verified on a parallel gripper, for which the grip force control was implemented by compressing soft finger with tactile feedback. Sintov *et al.* [12] used optimal control to solve the *gravity pivoting* control problem by linearizing the dynamics for one mode. They also designed a strategy to swing the object up above the desired angle. The main limitation for both work is the dependency on gravity, which makes it hard to recover from overshoot.

Pivoting is a typical example of nonprehensile manipulation (except [13]), where the object is manipulated without a firm grasp. Analysis of nonprehensile manipulation dates back to the 1980s. A more thorough list of nonprehensile manipulation can be found in [20, 21].

2.2 Friction Modeling

Friction determines the interaction between robots and grasped objects in pivoting [13, 7, 11]. The tribology community has extensive researches on precise friction modeling [22]. Static friction models treat friction as a memoryless function of contact normal force, contact sliding velocity and external force, [5]. More detailed static friction phenomena and modeling can be found in [5]. In the robotics community, Goyal analyzed the Coulomb friction in rigid body 2D planar sliding, described the relation between the wrench acting on the object and 3D twist of the object using *limit surface* concept. Zhou *et al.* proposed a polynomial approximation of the limit surface [23], and a method for fast identification from pushing experiments.

The discontinuity and lack of expressiveness of static friction models motivates dynamic friction modeling [5, 6, 4], which provides smooth friction behavior even during friction direction transitions. Dynamic friction models use one or more hidden state variables to describe microscopic asperities in contact [6, 4]. Complicated friction models provide a more precise description of friction phenomena. The cost is more effort and more data required for parameter estimation. In this work, we will stick to a static model while relying on hardware design to minimize unexpected dynamic frictional behavior.

3 Modeling

3.1 Robot Hardware

Fig. 2 shows our robot tailored for this task by emulating human operation. The wrist joint motor generates rotational torque and provides inertial force to the hand assembly. The top motor generate grip force through a lever mechanism. The bottom fingertip, which is mounted on a low-friction small-inertia shaft, contacts the object with high friction rubber and rotates with it. The rotational angles of the object is thus measured by an encoder on the shaft. The lower finger is installed on a loadcell to provide grip force feedback.

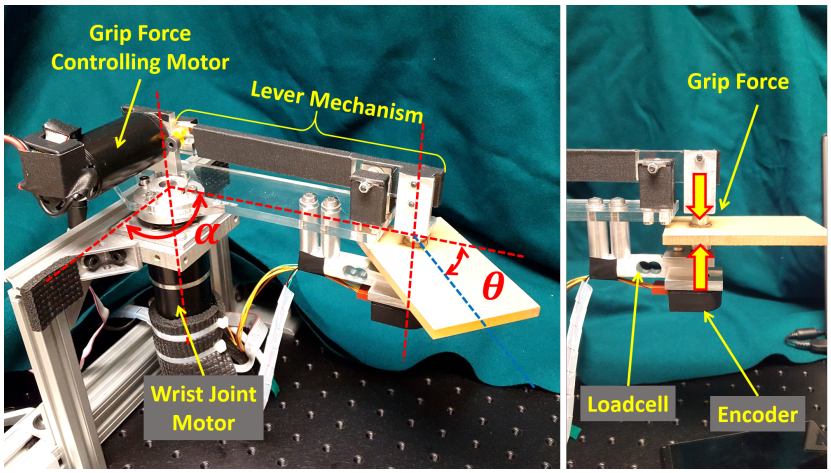

Fig. 2. The robot and gripper designed for dynamic pivoting.

The top finger provides frictional torque through a piece of hard fingertip. It is chosen to be hard and thin to minimize spring-like stiction behavior [5], which is reported as troublesome for pivoting in [9]. Large stiction makes it hard to predict when sliding will occur. The size of the fingertip is critical. A smaller contact area will result in a more flat limit surface [24], which makes rotation easier than slip. The fingertip should also be large enough to provide frictional torque in order to handle the object's momentum. It is also important to select the right material so that a non-trivial range of friction can be provided by the grip force. In our experiments, a 11mm-diameter round piece cut from a 0.8mm-thick Teflon sheet is used.

To drive the wrist joint, we choose a Maxon RE-40 DC motor (with a 4.3:1 gearbox) operated in current control mode with 0.8Nm maximum continuous torque output. The torsional friction in this joint is modeled and compensated as constant stiction plus viscous friction. The grip force is produced by a current controlled Maxon RE-36 DC motor. Through a lever mechanism, the motor

can provide a maximum of 40N grip force, while staying close to the wrist axis and contributing a small moment of inertia. There is a significant hysteresis nonlinearity in motor stall torque; hence we use a 5kg loadcell to provide grip force feedback, then close the loop with a PI plus feed-forward controller. Typical response time of the grip force control is around 25ms, which is limited by the latency in loadcell reading.

3.2 Two Link Model

The following assumptions are made on the pivoting robot shown in Fig. 2:

1. Dimensional/inertial properties of the robot and the object are known.
2. The robot wrist joint axis is parallel to gravity. The object always stays within the horizontal plane during motion. Consequently, the gravity does not affect the rotation of the robot or the object.
3. The object is initially grasped at rest, but our knowledge of the grasping position may not be exact.
4. The object may have translational slip during motion, but will not slip off the gripper.

Denote α as the wrist joint angle. Instead of coping with a known object with uncertain position, we model the contact as pin joint (call it *pivoting joint*, joint variable denoted by θ), and treat the object as an additional link whose inertia properties have uncertainty. Denote $\mathbf{x} = [\theta, \alpha]^T$ as the joint state vector. The Lagrange dynamics of the whole 2-DOF system are:

$$M(\mathbf{x})\ddot{\mathbf{x}} + C(\dot{\mathbf{x}}, \mathbf{x})\dot{\mathbf{x}} + N(\mathbf{x}) = \begin{pmatrix} \tau_f(\dot{\mathbf{x}}, N_f) \\ \tau \end{pmatrix}, \tag{1}$$

where the joint torque vector consists of wrist torque τ and contact frictional torque τ_f. For friction modeling we use Coulomb friction plus stiction, which is a trade-off between accurancy and simplicity. Then the frictional torque can be related to the contact normal force N_f by [5]:

$$\tau_f = \begin{cases} -\mu N_f \mathrm{sgn}(\dot{\theta}) & \text{if } \dot{\theta} \neq 0 \\ -F_e & \text{if } \dot{\theta} = 0 \text{ and } |F_e| \leq \mu N_f \\ -\mu N_f \mathrm{sgn}(F_e) & \text{otherwise} \end{cases}, \tag{2}$$

where F_e is the external torque [5] acting on the contact. Note the normal force is subjected to unilateral constraint:

$$N_f \geq N_f^{(\mathrm{low})} > 0 \tag{3}$$

Denote control vector as $\mathbf{u} = [N_f, \tau]^T$. We can express the hybrid dynamics (1) with a compact form:

$$\ddot{\mathbf{x}} = F(\mathbf{x}, \dot{\mathbf{x}}) + B(\mathbf{x}, \dot{\mathbf{x}})\mathbf{u}. \tag{4}$$

We suppress the arguments $\mathbf{x}, \dot{\mathbf{x}}, \ddot{\mathbf{x}}$ in what follows for conciseness. For slipping mode $|\dot{\theta}| \neq 0$, we have:

$$F = -M^{-1}(C+N), \quad B = B_{\text{Slipping}} := M^{-1} \begin{bmatrix} -\mu \operatorname{sgn}(\dot{\theta}) & 0 \\ 0 & 1 \end{bmatrix}. \tag{5}$$

The gain matrix B is of full rank, so feedback linearization is possible. Similarly, when $\dot{\theta} = 0$ and $|F_e| > \mu N_f$, the dynamics are still of the form in (4), but with:

$$B = B_{\text{ToSlip}} := M^{-1} \begin{bmatrix} -\mu \operatorname{sgn}(F_e) & 0 \\ 0 & 1 \end{bmatrix}. \tag{6}$$

During sticking, however, the system reduces to 1D. Denote m_c as the momentum of inertia of the whole assembly, the dynamics satisfies:

$$F = \mathbf{0}, \quad B = B_{\text{Sticking}} := \begin{bmatrix} 0 & 0 \\ 0 & m_c^{-1} \end{bmatrix} \tag{7}$$

Here the zeros are vectors of suitable size. In practice, we replace the condition $\dot{\theta} = 0$ by a range $|\dot{\theta}| < \xi$, where ξ describes the noise level in angular velocity measurement.

3.3 Uncertainty Analysis

Our experiment shows that there is a considerable amount of uncertainty in friction, which is a compound result of a simple friction model, non-perfect friction parameter estimation, and the noise in grip force control. This uncertainty directly affects the gain matrix B in (4). Another source of uncertainty is the grasping position. In our pin joint model, this uncertainty will affect the inertia matrix M in the Lagrange dynamics (1), which will eventually affect both F and B in (4). The influence of all other uncertainty sources, including measurement noise, can be modeled as an uncertainty in F. Denoting by $\hat{F}$ and $\hat{B}$ our estimation of F and B, respectively, we can describe the bounded uncertainty as:

$$\begin{array}{ll} \hat{F} = F + \Delta_F & |\Delta_F| \prec \delta_F \\ B = \Delta_B \hat{B} & |\Delta_B - I| \prec \delta_B. \end{array} \tag{8}$$

where $|\cdot|$, $\prec$ denote element-wise absolute value and inequality. $\delta_F \succ \mathbf{0}, \delta_B \succ \mathbf{0}$ are estimated error bounds. With this notation, the true dynamics (4) can be expressed by the estimated model with bounded uncertainty as:

$$\ddot{\mathbf{x}} = \hat{F}(\mathbf{x}, \dot{\mathbf{x}}) - \Delta_F + \Delta_B \hat{B}(\mathbf{x}, \dot{\mathbf{x}})\mathbf{u}. \tag{9}$$

Note that if Δ_B has non-zero off-diagonal component we can decompose it into diagonal and off-diagonal terms, $\Delta_B = I_D + O_D$. Then, move the off-diagonal terms out of gain matrix:

$$\ddot{\mathbf{x}} = \hat{F} - (\Delta_F - O_D \hat{B}\mathbf{u}) + I_D \hat{B}\mathbf{u},$$

and treat the quantity inside the parentheses as the new Δ_F, which is still bounded. Consequently, we consider Δ_B to be diagonal from now on:

$$\Delta_B = \begin{bmatrix} d_{b1} & 0 \\ 0 & d_{b2} \end{bmatrix}, d_{b1}, d_{b2} > 0. \tag{10}$$

It is not trivial to estimate an error bound on $\hat{F}$ or $\hat{B}$, as the error is a compound result of multiple sources of uncertainty. Instead, we treat them as parameters and tune them according to experimental results.

4 Robust Controller Design

4.1 Robust Controller Design Within a Continuous Mode

Within any certain mode, the system is continuous with uncertainties described in Section 3.3. Before considering constraints, we can use the sliding mode control (SMC) [25] to solve the unconstrained problem, for its ability to converge under bounded uncertainty. Denote $\mathbf{x}_r(t)$ as a smooth reference state trajectory, the control task is to make the tracking error $\mathbf{x}(t) - \mathbf{x}_r(t)$ converge to zero. The 2-D sliding mode $\mathbf{s} = [s_1, s_2]^T$ is defined as:

$$\mathbf{s}(t) = G_D\dot{\tilde{\mathbf{x}}}(t) + G_P\tilde{\mathbf{x}}(t) + G_I\int_0^t \tilde{\mathbf{x}}(\tau)d\tau, \tag{11}$$

where $\tilde{\mathbf{x}}(t) = \mathbf{x}(t) - \mathbf{x}_r(t)$ is the state tracking error, and G_P, G_I, and G_D are diagonal positive definite coefficient matrices. When the system stays on the *sliding surface* $\mathbf{s} = \mathbf{0}$, equation (11) indicates that $\tilde{\mathbf{x}}(t)$ will converge to zero exponentially. Thus the control problem for the original system is equivalent to the problem of stabilizing $\mathbf{s}$, which is only a first-order system described by:

$$\dot{\mathbf{s}} = G_D F + \tilde{G} + G_D B\mathbf{u}, \quad \tilde{G} := -G_D\ddot{\mathbf{x}}_r + G_P\dot{\tilde{\mathbf{x}}} + G_I\tilde{\mathbf{x}} \tag{12}$$

Use the following Lyapunov function:

$$V = \frac{1}{2}\mathbf{s}^T\mathbf{s}, \tag{13}$$

And choose the controller structure to be a feedback linearization term plus a robust control term: (the measured $\hat{B}$,$\hat{F}$ are described in (8))

$$\mathbf{u} = (G_D\hat{B})^{-1}(-G_D\hat{F} - \tilde{G} - K\,\mathrm{sgn}(\mathbf{s})), \tag{14}$$

where K is the gain matrix: $K = \begin{bmatrix} k_1 & 0 \\ 0 & k_2 \end{bmatrix} \succ 0$, Now we can express $\dot{V}$ as:

$$\begin{aligned} \dot{V} &= \mathbf{s}^T\dot{\mathbf{s}} \\ &= \mathbf{s}^T\left(-G_D\Delta_F + G_D(I - \Delta_B)\hat{F} + (I - \Delta_B)\tilde{G}\right) - \mathbf{s}^T\Delta_B K\mathrm{sgn}(\mathbf{s}) \end{aligned} \tag{15}$$

The function V becomes a Robust Control Lyapunov Function (RCLF) and guarantees convergence if there exists $\mathbf{u}$ to make its derivative negative under all possible uncertainties:

$$\dot{V} < -\eta||\mathbf{s}||, \qquad \forall|\Delta_F| \prec \delta_F, |\Delta_B - I| \prec \delta_B. \tag{16}$$

This is called *the sliding condition* in sliding control literature [25], as it ensures $\mathbf{s}$ converges to sliding surface exponentially. The sliding condition is satisfied if

$$D_{\text{low}}\mathbf{k} > C_{\text{up}}. \tag{17}$$

where $\mathbf{k} = [k_1, k_2]^T$, $D_{\text{low}}, C_{\text{up}}$ are lower bound and upper bound of

$$\begin{aligned} D &= \begin{bmatrix} |s_1|d_{b1} \\ |s_2|d_{b2} \end{bmatrix}^T, \\ C &= \mathbf{s}^T \left(-G_D\Delta_F + G_D(I - \Delta_B)\hat{F} + (I - \Delta_B)\tilde{G} \right) + \eta||\mathbf{s}||. \end{aligned} \tag{18}$$

Here we use the fact that G_D, Δ_B are diagonal to simplify the derivation. The bound can be obtained by linear programming over Δ_F and Δ_B. In traditional sliding control, we solve equation (17) for $\mathbf{k}$, calculate controls $\mathbf{u}$ from (14). However, in pivoting we also need to consider control saturation constraints:

$$\begin{aligned} &N_f^{(\text{low})} < N_f < N_f^{(\text{high})}, \\ &\tau^{(\text{low})} < \tau < \tau^{(\text{high})}. \end{aligned} \tag{19}$$

where the *positive lower bound* N_{low} is causing problem. In simulation the controller often produces negative grip force, and the control would fail if we truncate grip force to satisfy saturation constraints. Instead of direct truncation, we need to leverage wrist rotation more when grip force can not attain a desired value, i.e. find a solution to for both (17) and (19). Unfortunately, the two constraints together are infeasible, if we do not have a tight uncertainty bound in Δ_B, Δ_F. In practice we enforce (17) by soft constraint and solve a constrained optimization at each time step, similar with the optimization performed in [26]. We solve for the two-dimensional gain $\mathbf{k}$ by:

$$\min_{\mathbf{k}} \quad (D_{\text{low}}\mathbf{k} - C_{\text{up}})^2 + w\mathbf{k}^T\mathbf{k}, \tag{20}$$

with (19) as the only constraint. The second term is a regularization term. From (14), we know $\mathbf{u}$ is linear in gain vector $\mathbf{k}$. Hence, the saturation constraints are linear on $\mathbf{k}$. Therefore, we end up with a quadratic programming problem that can be efficiently solved by an off-the-shelf QP solver. The overall computation time, including solving the LP and QP, is less than 1ms for each control loop.

The optimization formulation above sacrifices robust convergence guarantee for feasibility. However, in experiments we still obtain good convergence, indicating the worst case guarantee is unnecessary in our case.

4.2 Control Strategy Among Different Modes

We design one controller for each mode. A such controller will not make sense if it drives the system to any other modes. This could happen when the pivoting velocity $\dot{\theta}$ equals zero, as shown in equation (2). Depending on the external torque F_e, the contact dynamics can end up in one of three possible modes:

- Rotating with $\ddot{\theta} > 0$, if $F_e > \mu N_f$;
- Rotating with $\ddot{\theta} < 0$, if $F_e < -\mu N_f$;
- Sticking, $\ddot{\theta} = 0$, if $|F_e| < \mu N_f$.

To resolve this ambiguity, we solve each of the three modes with the condition above as additional constraints. Then we just pick the solution with optimal cost. In hybrid systems theory, the additional condition is called *guard condition* [27]. Note F_e is linear in $\mathbf{u}$, thus the guard conditions are linear in $\mathbf{k}$, and the problem is still quadratic programming.

The last issue is when to stop the controller. We observe in experiments that the closed-loop system has small-amplitude oscillations around the goal. To stop the oscillation, we set the goal region to be $|\theta - \theta_{\text{goal}}| < \sigma$, and stop the controller as soon as the object stops within this region. The overall algorithm at each control time step is described as follows:

1. If $|\dot{\theta}| > \xi$, solve the corresponding mode for control.
2. While $|\dot{\theta}| <= \xi$,
   (a) If $|\theta - \theta_{\text{goal}}| < \sigma$, stop the control loop and apply the maximum grip force with zero wrist torque.
   (b) Otherwise, solve the three possible modes under guard condition respectively, and pick the one with the best cost value.

5 Experiments

The proposed algorithm is implemented on the hardware described in Section 3.1. The robust control loop runs at 50Hz. The object to be rotated is an acrylic board with a protective paper cover.

5.1 System Identification and Parameter Tuning

Robot mass	700g	Robot moment of inertia	$8.9 \times 10^{-3}\text{kgm}^2$
Object mass	44g	Object moment of inertia	$8.96 \times 10^{-5}\text{kgm}^2$
Length of wrist link	0.16m	Contact friction coefficient μ	4.5×10^{-4}m
Grip force range	$4\text{N} \sim 15\text{N}$	Wrist joint torque range	$-0.5\text{Nm} \sim 0.5\text{Nm}$

Table 1. Physical properties of the robot and the object.

The inertia parameters of the robot are identified offline from torque-speed profile. To measure the friction coefficient between the object and the finger, we

fix the wrist joint and apply a certain grip force on the object. Then we give the object an initial rotational velocity and record the deceleration curve. The friction coefficient estimated are shown in Fig. 3. An affine relation is fitted, with a rate representing the Coulomb friction coefficient. Physical parameters and actuation constraints are listed in table 5.1. Note all frictional coefficients are torsional.

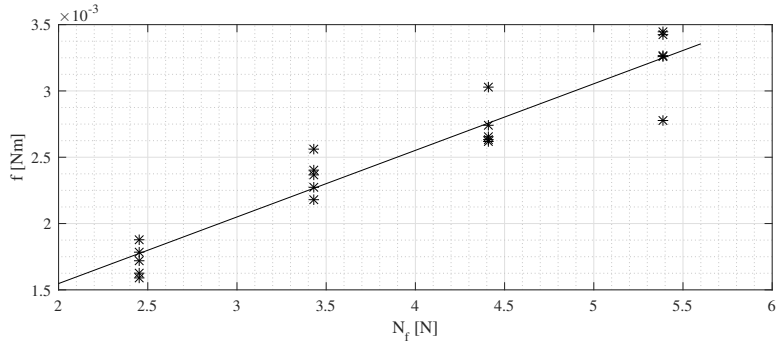

Fig. 3. Measured torsional friction f under different grip forces N_f.

Now we briefly explain how to tune parameters. δ_B can be estimated from friction measuring data, and here we use $\delta_B = \begin{bmatrix} 0.4 & \\ & 0.1 \end{bmatrix}$. The performance is not sensitive to η, we pick $\eta = 5$. Next, start with $\delta_F = 0$, we firstly tune the gains G_P, G_I, G_D as if we are tuning a normal PID controller. When performance is peaked, go back to tune δ_F. Repeat the last two steps until satisfactory performance is obtained.

5.2 Experiment I: Pivoting under Grasping Position Uncertainty

In real-life manipulation, the object may not be grasped exactly at the expected position. The ability to endure grasping position uncertainty is crucial to pivoting control. Here we implement and compare our method with two baselines: The first baseline controller is based on partial feedback linearization (PFL), which is a typical approach in the passive manipulator literature [14–18]. In this controller, only wrist joint torque is used as control. The control is chosen such that the dynamics of the passive joint (i.e. the object) is linear and stable, while the stability of the wrist joint dynamics is determined by the zero dynamics of the system, which can be shown to be stable using center manifold theorem if we ignore friction [14]. In our simulation, the approach converges to the goal if there is no friction and no slip. However the inertia force generated on the object is usually very low. If we add friction, the inertia force is not able to overcome stiction, the controller would diverge by keeping accelerating wrist joint. The phenomenon is verified in experiments. The second baseline is a robust controller that only uses wrist joint torque as control. It extends the first controller

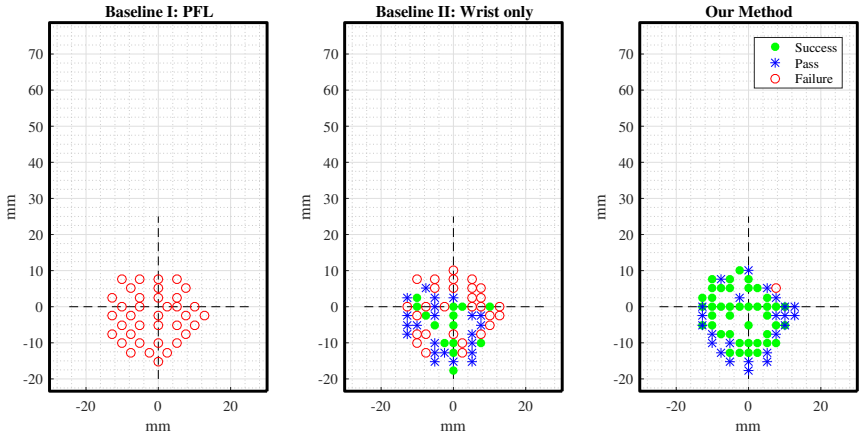

Fig. 4. Results of experiment I. Each dot represents the actual initial grasping position with respect to the object (the outer solid line frame) for one pivoting trail, while the cross of dotted lines denotes the nominal grasping position. A green solid circle denotes a success, a blue star denotes a pass, and a red circle denotes a failure.

in that friction (and its uncertainty) is explicitly handled. Here we set the target object rotation to be $\theta = 1\,\text{rad}$, starting from zero initial condition $\theta = \alpha = 0$. The reference trajectory θ_{ref} in $\mathbf{x}_{\text{ref}}$ is generated by simulating PID control on an integrator, so we can tune its shape. α_{ref} in $\mathbf{x}_{\text{ref}}$ is simply set to zero, as we expect the wrist to stay close to the origin and move gently. The two baselines do not utilize grip force, thus we set grip force to the minimal possible value (4N) to make them work better.

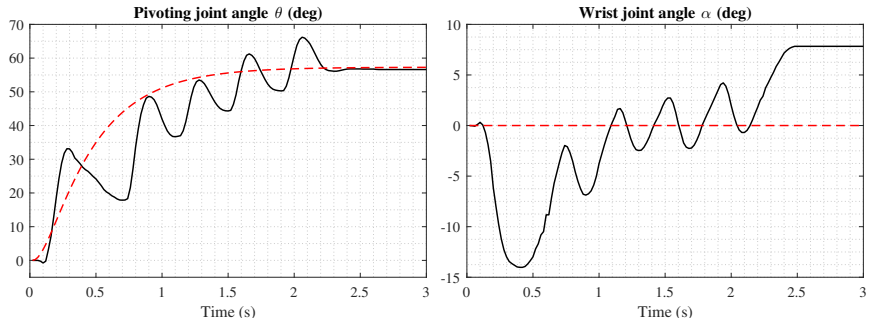

Fig. 5. The reference (dashed line) and response (solid line) trajectories of object orientation θ and robot wrist angle α of our method.

We perform the experiment multiple times with different initial positions offset unknown to the controller. The results are plotted in Fig. 4. A success is defined as converging and stopping in the target region $[0.95, 1.05]$ within 4 seconds. A pass means the object motion is converging, but not fast enough to stop within 4s. Failure means the trail diverged. Our full controller almost converges all the time and outperforms the other two approaches. Fig. 5 shows a typical response

for our full controller. Note that during pivoting, the θ converges to the desired region with a steady-state error less than 0.05rad, while the wrist joint stays close to the origin (within about 0.25rad).

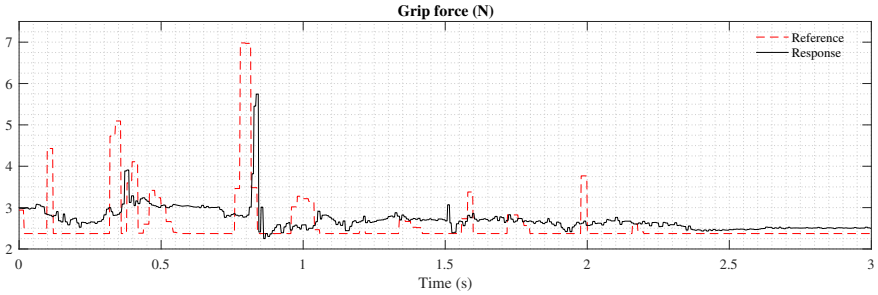

Fig. 6. The grip force control in pivoting.

The calculated grip force and the loadcell feedback are shown in Fig. 6, with notable tracking error. The main source of error is the noise generated from fast motion. In our grip force control test, the error grows immediately as the object rotates. Although the lower-level force control is not perfect, this source of control still appears to be crucial to the overall stability.

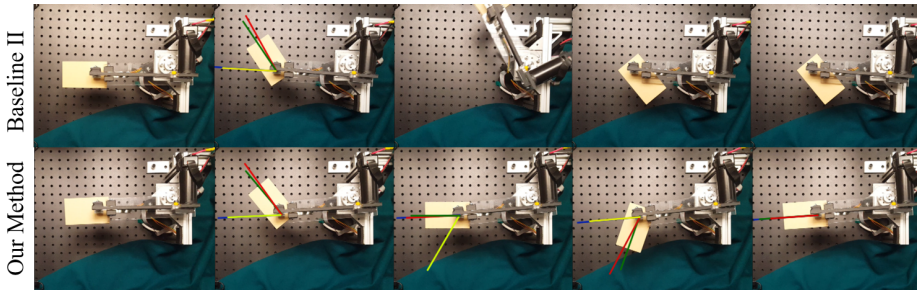

Fig. 7. Snapshots of consecutive pivoting experiments comparing wrist only controller (top) and full controller (bottom). The blue, green, red and yellow lines are hand orientation, object orientation, goal orientation and the next goal, respectively.

The ability to tolerate grasping position uncertainty becomes important in tasks where multiple pivots are performed consecutively, as the slips will accumulate. Starting from a precise initial grasping position (error < 0.3mm), the controller with grip force control is able to perform at least four pivots stably in a row, while the controller without grip force control will diverge before finishing the second pivot, as shown in Fig. 7. We omit partial feedback linearization controller to save space, as it never works. See attached video for more details.

5.3 Experiment II: Disturbance Recovery

Our closed-loop controller is able to recover from unexpected disturbances. To illustrate this, we run the controller with goal at the origin, and directly perturb the object through external intervention. The controller with both wrist torque and grip force control can always recover from disturbance and converge back to the origin, while the one without grip force control will diverge quickly. The results are shown in Fig. 8. Again we omit partial feedback linearization controller to save space, as it diverges immediately after perturbation. See the attached video for all three experiments.

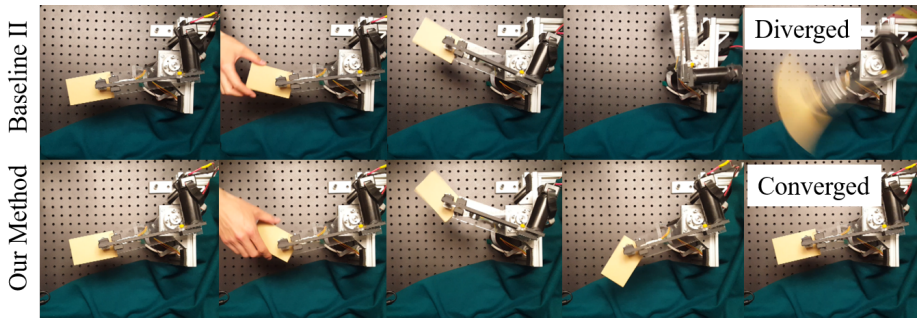

Fig. 8. Snapshots of pivoting under disturbance, comparing wrist only controller (top) and full controller (bottom)

5.4 Discussion

An interesting phenomenon observed from our experiments is the small-amplitude oscillation shown in Fig. 5 and Fig. 6. The oscillation has a pattern sometimes observed in human pivoting. This is partly due to the fact that the robust controller, or a human, tries to move the object towards the goal even in the worst possible friction. This will make it hard to avoid overshoot within one control time step. The observation suggests a faster control loop with lower latency is likely to reduce the oscillation.

6 Conclusions and Future Work

We have performed robust dynamic pivoting driven by inertial force and grip force, and described the robust control algorithm being used. The work helps us better understand how to cope with friction in manipulation tasks. It is worth noting that a coarse grip force control can significantly improve the stability of the closed-loop pivoting system. The experiment results also help us better understand how humans cope with friction. We use a low control frequency (50Hz) on a highly dynamic motion. This agrees with the human case where control frequency is also low because of slow nerve conduction velocity. The

auto-generated oscillation pattern is similar to human pivoting strategy, which may suggest the importance of incorporating feedback information and actively recover from error.

We believe a precise, less noisy grip force controller with lower latency is likely to improve the performance of pivoting. Our gripper only approximates a parallel gripper for objects of a certain thickness, which is another limitation to be resolved in the future. Our algorithm behaves greedily in terms of friction mode switching. A higher level planning on the sequence of modes may bring further performance improvement. Finally, we are also interested in exploring learning and adaptive control strategies that can handle more general problems, where knowledge of the object inertia property and friction coefficient is not fully available.

7 Acknowledgment

We appreciate Francisco E. Viña B., Yiannis Karayiannidis and François R. Hogan for insightful discussions and suggestions. This material is based upon work supported by the National Science Foundation under Grant No. 1662682.

References

1. N. C. Dafle, A. Rodriguez, R. Paolini, B. Tang, S. S. Srinivasa, M. Erdmann, M. T. Mason, I. Lundberg, H. Staab, and T. Fuhlbrigge, "Extrinsic dexterity: In-hand manipulation with external forces," in *2014 IEEE International Conference on Robotics and Automation (ICRA)*, 2014, pp. 1578–1585.
2. A. Holladay, R. Paolini, and M. T. Mason, "A general framework for open-loop pivoting," in *2015 IEEE International Conference on Robotics and Automation (ICRA)*, pp. 3675–3681.
3. C. Canudas, K. Astrom, and K. Braun, "Adaptive friction compensation in dc-motor drives," *IEEE Journal of Robotics and Automation*, vol. 3, no. 6, pp. 681–685, 1987.
4. C. C. De Wit, H. Olsson, K. J. Astrom, and P. Lischinsky, "A new model for control of systems with friction," *IEEE Transactions on Automatic Control*, vol. 40, no. 3, pp. 419–425, 1995.
5. H. Olsson, K. J. Åström, C. C. De Wit, M. Gäfvert, and P. Lischinsky, "Friction models and friction compensation," *European journal of control*, vol. 4, no. 3, pp. 176–195, 1998.
6. B. Armstrong-Hélouvry, P. Dupont, and C. C. De Wit, "A survey of models, analysis tools and compensation methods for the control of machines with friction," *Automatica*, vol. 30, no. 7, pp. 1083–1138, 1994.
7. J. Shi, J. Z. Woodruff, and K. M. Lynch, "Dynamic in-hand sliding manipulation," in *2015 IEEE/RSJ International Conference on Intelligent Robots and Systems*, 2015, pp. 870–877.
8. B. Vina, E. Francisco, Y. Karayiannidis, K. Pauwels, C. Smith, and D. Kragic, "In-hand manipulation using gravity and controlled slip," in *2015 IEEE/RSJ International Conference on Intelligent Robots and Systems*, pp. 5636–5641.

9. F. E. Vi, Y. Karayiannidis, C. Smith, D. Kragic *et al.*, "Adaptive control for pivoting with visual and tactile feedback," in *2016 IEEE International Conference on Robotics and Automation (ICRA)*, pp. 399–406.
10. A. Rao, D. J. Kriegman, and K. Y. Goldberg, "Complete algorithms for feeding polyhedral parts using pivot grasps," *IEEE Transactions on Robotics and Automation*, vol. 12, no. 2, pp. 331–342, 1996.
11. D. L. Brock, "Enhancing the dexterity of a robot hand using controlled slip," in *1988 IEEE International Conference on Robotics and Automation*, 1988, pp. 249–251.
12. A. Sintov, O. Tslil, and A. Shapiro, "Robotic Swing-Up regrasping manipulation based on the ImpulseMomentum approach and cLQR control," *Ieee T Robot*, vol. 32, no. 5, pp. 1079–1090, 2016.
13. N. Chavan-Dafle and A. Rodriguez, "Prehensile pushing: In-hand manipulation with push-primitives," 2015.
14. M. W. Spong, "The swing up control problem for the acrobot," *Control Systems, IEEE*, vol. 15, no. 1, pp. 49–55, 1995.
15. M. W. Spong and D. J. Block, "The Pendubot: a mechatronic system for control research and education," in *Proceedings of the 34th IEEE Conference on Decision and Control*, vol. 1, 1995, pp. 555–556 vol.1.
16. A. De Luca, R. Mattone, and G. Oriolo, "Stabilization of an underactuated planar 2r manipulator," *International Journal of Robust and Nonlinear Control*, vol. 10, no. 4, pp. 181–198, 2000.
17. Y. Nakamura, T. Suzuki, and M. Koinuma, "Nonlinear behavior and control of a nonholonomic free-joint manipulator," *IEEE Transactions on Robotics and Automation*, vol. 13, no. 6, pp. 853–862, 1997.
18. A. De Luca and G. Oriolo, "Trajectory planning and control for planar robots with passive last joint," *The International Journal of Robotics Research*, vol. 21, no. 5-6, pp. 575–590, 2002.
19. L. Gaul and R. Nitsche, "Friction control for vibration suppression," *Mechanical Systems and Signal Processing*, vol. 14, no. 2, pp. 139–150, 2000.
20. K. M. Lynch and M. T. Mason, "Stable pushing: Mechanics, controllability, and planning," *The International Journal of Robotics Research*, vol. 15, no. 6, pp. 533–556, 1996.
21. ——, "Dynamic nonprehensile manipulation: Controllability, planning, and experiments," *The International Journal of Robotics Research*, vol. 18, no. 1, pp. 64–92, 1999.
22. B. Armstrong-Hélouvry, P. Dupont, and C. Canudas de Wit, "A Survey of Models, Analysis Tools and Compensations Methods for the Control of Machines with Friction," *Automatica*, vol. 30, no. 7, pp. 1083–1138, 1994.
23. J. Zhou, R. Paolini, J. A. Bagnell, and M. T. Mason, "A convex polynomial force-motion model for planar sliding: Identification and application," in *2016 IEEE International Conference on Robotics and Automation (ICRA)*, 2016, pp. 372–377.
24. S. Goyal, A. Ruina, and J. Papadopoulos, "Planar sliding with dry friction part 1. limit surface and moment function," *Wear*, vol. 143, no. 2, pp. 307–330, 1991.
25. J.-J. E. Slotine, W. Li *et al.*, *Applied nonlinear control*. Prentice-Hall Englewood Cliffs, NJ, 1991, vol. 199, no. 1.
26. M. Spong, J. Thorp, and J. Kleinwaks, "The control of robot manipulators with bounded input," *IEEE Transactions on Automatic Control*, vol. 31, no. 6, pp. 483–490, 1986.
27. R. Goebel, R. G. Sanfelice, and A. R. Teel, "Hybrid dynamical systems," *IEEE Control Systems*, vol. 29, no. 2, pp. 28–93, 2009.